Locally translated mTOR controls axonal local translation in nerve injury

Marco Terenzio[1], **Sandip Koley**[1], **Nitzan Samra**[1], **Ida Rishal**[1], **Qian Zhao**[2,†], **Pabitra K. Sahoo**[3], **Anatoly Urisman**[2], **Letizia Marvaldi**[1], **Juan A. Oses-Prieto**[2], **Craig Forester**[2,4], **Cynthia Gomes**[3,‡], **Ashley L. Kalinski**[3,§], **Agostina Di Pizio**[1], **Ella Doron-Mandel**[1], **Rotem Ben-Tov Perry**[1], **Indrek Koppel**[1], **Jeffery L. Twiss**[3,5], **Alma L. Burlingame**[2], and **Mike Fainzilber**[1,*]

[1]Department of Biomolecular Sciences, Weizmann Institute of Science, Rehovot 76100, Israel

[2]Department of Pharmaceutical Chemistry, University of California, San Francisco, CA 94158, U.S.A

[3]Department of Biological Sciences, University of South Carolina, Columbia, SC 29208, U.S.A

[4]Division of Pediatric Allergy, Immunology & Bone Marrow Transplantation, University of California, San Francisco, CA 94158, U.S.A

[5]Dept of Neurobiology and Anatomy, Drexel University College of Medicine, Philadelphia, PA 19129, U.S.A

Abstract

How is protein synthesis initiated locally in neurons? We found that mTOR was activated and then upregulated in injured axons, owing to local translation of mTOR mRNA. This mRNA was transported into axons by the cell size regulating RNA-binding protein nucleolin. Furthermore, mTOR controlled local translation in injured axons. This included regulation of its own translation and that of retrograde injury signaling molecules such as importin β1 and STAT3. Deletion of the mTOR 3′UTR in mice reduced mTOR in axons and decreased local translation after nerve injury. Both pharmacological inhibition of mTOR in axons and mTOR 3′UTR deletion decreased proprioceptive neuronal survival after nerve injury. Thus, mRNA localization enables

[*]Correspondence to: mike.fainzilber@weizmann.ac.il.
[†]Current address: Department of Applied Biology and Chemical Technology, Hong Kong Polytechnic University, Hong Kong.
[‡]Current address: Department of Anatomical Sciences and Neurobiology, University of Louisville, KY 40202, U.S.A.
[§]Cell and Developmental Biology, University of Michigan Medical School, 109 Zina Pitcher Pl, Ann Arbor, MI 48188, U.S.A.

spatiotemporal control of mTOR pathways regulating local translation and long range intracellular signaling.

Local translation enables spatiotemporal specificity in cell functions (1, 2) such as the neuronal response to axon injury (3, 4) or regrowth of injured axons (5, 6). However apart from a requirement for intraxonal calcium (7), the mechanisms that regulate local protein synthesis in axons are largely unknown. mTOR, the mechanistic Target of Rapamycin, is a central regulator of translation (8), neuronal regeneration (9–12), and protein synthesis in neurons (13–16). We examined mTOR signaling in sciatic nerve (SN) versus dorsal root ganglia (DRG) after axonal injury, and found differential phosphorylation of both mTOR and associated signaling components (Fig. 1A, B, Table S1). This suggested a specific role for mTOR in the early injury response in axons. We verified mTOR S2448 phosphorylation (17) in axons by immunostaining, observing significant elevation within axons at 3 hr after injury with a return to baseline at 12 hr (Fig. 1C, D). We also observed that phosphorylation levels of EiF4b (S406), Akt (S473), S6 kinase (S6K, T389), and ribosomal protein S6 (S240/244), all well-known effectors and regulators of mTOR signaling, increased rapidly after injury (Fig. 1E). Typically, Eif4b is activated in response to mTORC1, while Akt plays a role in both mTORC1 and mTORC2 signaling (8, 18), hence both mTOR complexes are activated locally by axonal injury.

We used the mTOR inhibitor torin-1 (Fig. S1A–C) to examine functions of local mTOR activation in nerve injury. Injection of torin-1 at the injury site prior to a conditioning SN lesion (19) reduced the subsequent lesion-induced axon outgrowth in culture (Fig. S1D, E). Neuron numbers recovered from torin-1 treated animals were also reduced (Fig. S1F), so we examined the effects of SN torin-1 injection on proprioceptive neuron survival in DRG in vivo. Injecting torin-1 in the nerve concomitantly with injury reduced proprioceptive neuron numbers in the corresponding DRG (Fig. 1F, G), supporting a role for axonal mTOR activation in neuronal injury response and survival. Examination of SN mTOR expression revealed surprisingly low levels of mTOR protein in axons prior to injury. There was a marked elevation of axonal mTOR in the vicinity of the lesion site up to 9 hr post-injury, followed by a decline back to baseline levels (Figs 2A and S2A). Upregulation of mTOR in injured axons was further confirmed by immuno-electron microscopy (EM) on SN sections (Fig. S2B).

The time frame of mTOR elevation in axons suggested it might be synthesized locally. We examined this possibility by biotinylation of nascent synthesized proteins tagged with the puromycin derivative O-propargyl-puromycin (OPP) (20). We performed OPP incubation and biotinylation in rat nerve segments ex vivo followed by axoplasm extraction (21) and precipitation with streptavidin (SA). Immunoblots of SA precipitates revealed robust de novo synthesis of mTOR, similar to that of importin β1, a well-established locally synthesized protein (22) (Fig. 2B). Immunostaining on mouse SN segments incubated ex vivo with the translation inhibitor cycloheximide revealed inhibition of axonal mTOR upregulation (Fig. S2C, D), and fluorescent in situ hybridization (FISH) showed robust granular signals for mTOR mRNA in axons (Fig. S2E). Direct visualization of de novo synthesized mTOR by puromycin labeling combined with a proximity ligation assay

revealed robust signal for de novo synthesis of mTOR in sensory axons in culture (Fig. S3A–C). mTOR axonal upregulation in nerve segments ex vivo and in culture was torin-1 sensitive (Fig. 2C, D and Fig. S3A–C), indicating that it is controlled by mTOR itself. Finally, mTOR upregulation after injury was mirrored by a decrease in axonal PTEN (Fig. S3D, E), a functional mTOR antagonist.

A complex comprising the RNA-binding protein (RBP) nucleolin and the kinesin motor Kif5A traffics importin β1 mRNA to axons (23). We tested for mTOR mRNA association with this complex by quantitative RT-PCR on immunoprecipitates of nucleolin or Kif5A from SN axoplasm. Indeed, mTOR mRNA was robustly co-precipitated with both nucleolin and Kif5A (Figs 2E and S4A, B). Furthermore, we observed significant colocalization of mTOR mRNA with nucleolin protein by combining FISH with immunostaining on sensory axons (Fig. 2F, G). Finally, restriction of nucleolin to neuronal somata by pre-treatment of neuronal cultures with the DNA aptamer AS1411 (23) reduced mTOR mRNA in axons while increasing it in cell bodies (Figs 2H and S4C, D), confirming that mTOR mRNA is transported to axons by the RBP nucleolin.

To assess the overall impact of mTOR on local translation in axons, we carried out puromycin labeling on SN segments preincubated with anisomycin, a general protein synthesis inhibitor, or with torin-1. We quantified puromycin incorporation into axonal proteins by immunostaining (Fig. 3A, B), and by capillary immuno-electrophoresis of axoplasm (Fig. 3C, D). Torin-1 effectively inhibited axonal protein synthesis to a similar degree as anisomycin (Fig. 3B, D). We then used OPP to characterize the ensemble of de novo synthesized proteins in axon injury by mass spectrometry (MS). SN segments were pre-incubated ex vivo with vehicle, anisomycin or torin-1, and then pulsed with OPP before axoplasm extraction and biotinylation (Fig. S5A). Efficiency of the reactions was assessed by immunoblotting with SA-HRP (Fig. 3E). A cohort of approximately 550 proteins was identified after affinity purification and MS, of which 234 were impacted equivalently by anisomycin or torin-1 pretreatments (Figs 3F and S5B, Table S2). Almost 80% of the torin-1 sensitive candidates were shared with the largest known translatome dataset of mTOR-regulated survival-promoting mRNAs (24, 25) (Fig. S5C). The mTOR-dependent axonally synthesized proteins included many known axonal injury response proteins (26) (Table S2), leading us to test the effect of torin-1 on injury-induced axonal upregulation of STAT3 (Fig. 3G, H), importin β1 (Fig. S5D, E), and vimentin (Fig. S5F, G). Locally translated STAT3 is phosphorylated in sensory axons as a retrograde survival signal (27), so we also tested the effect of torin-1 on phospho-STAT3 (Fig. 3G, H). Indeed, torin-1 effectively inhibited the localized axonal elevation of all the tested injury-signaling proteins, indicating that local translation for retrograde injury signaling is controlled by mTOR in sensory axons.

The findings above suggest that axonal localization of mTOR mRNA enables subcellular regulation of axonal protein synthesis. Localization motifs are often located in the 3′ untranslated regions (3′UTR) of axonal mRNAs (28) and axonal localization was previously reported for the mTOR 3′UTR (15). We sequenced 3′ RACE PCR products and identified a single major mTOR 3′UTR sequence as expected from genome annotation. The mTOR 3′UTR indeed effectively localized GFP mRNA to axons in transfected neurons (Fig. S6A, B). We then removed most of the 3′UTR sequence from the mTOR locus using CRISPR/

Cas9 gene editing (Fig. S6C, Table S3) without affecting the open reading frame or other elements of the gene. We verified that the segment targeted for deletion (mTOR 3′UTR 54–789) contained axon-localizing capacity, while segments predicted to be retained in the mutant mouse lacked axon-localizing capacity (mTOR 3′UTR 1–69, 774–825, Fig. S6A, B). mTOR 3′UTR null mice were viable, and 3′RACE analyses on homozygous null DRG neurons confirmed the deletion (Fig. S6D).

FISH analyses on SN sections revealed a significant reduction in axonal mTOR mRNA levels in vivo in the SN of mTOR 3′UTR null mice (Figs 4A, B and S6E), with no significant changes in stability or half-life of mTOR mRNA or protein (Fig. S7). Ex vivo incubation of mTOR 3′UTR null SN segments revealed a large reduction in injury-induced mTOR protein upregulation as compared to wild-type (Fig. 4C, D). Cultures of 3′UTR null neurons revealed little or no change in mTOR protein levels in the soma, while mTOR protein levels in the growth cones and axon tips were significantly reduced (Fig. S8A, B). These subcellular effects on mTOR protein upregulation were mirrored in mTOR downstream signaling, with no change in phospho-S6 levels in somata of 3′UTR null neurons, in contrast to a marked deficit in phospho-S6 upregulation in injured axons from the mutant mice (Fig. S8C, D).

We then examined effects of the mTOR 3′UTR deletion on axonal protein synthesis and on the mTOR-dependent injury response in lesioned DRG neurons. Puromycinylation experiments in SN segments ex vivo showed a clear reduction in puromycin incorporation in mTOR 3′UTR null axons (Figs 4E, F and S9A–D). SN injury in mutant mice lead to reductions in L4 DRG proprioceptive neuron numbers seven days later to a similar degree as we previously observed for torin-1 injection concomitantly with injury (Figs 4I and S9E). We tested whether the observed effects were indeed due to loss of mTOR upregulation in injured axons by injecting recombinant mTOR protein to the nerve concomitantly with injury. Exogenously supplied mTOR protein indeed rescued both local axonal translation (Fig. 4G, H) and neuronal survival (Figs 4I and S9E) in the mutant mice. Thus, removal of the mTOR 3′UTR reduces axonal localization of mTOR mRNA and attenuates local elevation of mTOR protein in injured axons. Subcellular reduction in axonal mTOR affects overall local protein synthesis in injured axons, and reduces the survival of lesioned neurons.

Maintenance of a latent and silent pool of mTOR in mRNA form in axons enables rapid and local upregulation of protein synthesis upon need. The linkage of mTOR mRNA transport to nucleolin likely explains nucleolin regulation of subcellular protein synthesis in cell size regulation (23). Regulation of mTOR pathways via mRNA localization may impact on many aspects of neuronal physiology apart from injury, because localized changes in mTOR activity affect diverse processes, including viral latency (29), autophagy (30), and synaptic plasticity (31). Intracellular localization of mTOR at the protein level is well established in non-neuronal cells (32–34). mTOR localization at the RNA level provides an additional mode of spatiotemporal regulation of its pathways, with potentially broad physiological implications.

Supplementary Material

Refer to Web version on PubMed Central for supplementary material.

Acknowledgments

References

1. Rangaraju V, Tom Dieck S, Schuman EM. Local translation in neuronal compartments: how local is local? EMBO Rep. 18:693–711.2017; [PubMed: 28404606]

2. Terenzio M, Schiavo G, Fainzilber M. Compartmentalized signaling in neurons: from cell biology to neuroscience. Neuron. 96:667–679.2017; [PubMed: 29096079]

3. Hanz S, et al. Axoplasmic importins enable retrograde injury signaling in lesioned nerve. Neuron. 40:1095–1104.2003; [PubMed: 14687545]

4. Perry RB, et al. Subcellular knockout of importin beta1 perturbs axonal retrograde signaling. Neuron. 75:294–305.2012; [PubMed: 22841314]

5. Zheng JQ, et al. A functional role for intra-axonal protein synthesis during axonal regeneration from adult sensory neurons. J Neurosci. 21:9291–9303.2001; [PubMed: 11717363]

6. Donnelly CJ, et al. Limited availability of ZBP1 restricts axonal mRNA localization and nerve regeneration capacity. EMBO J. 30:4665–4677.2011; [PubMed: 21964071]

7. Yudin D, et al. Localized regulation of axonal RanGTPase controls retrograde injury signaling in peripheral nerve. Neuron. 59:241–252.2008; [PubMed: 18667152]

8. Fonseca BD, et al. The ever-evolving role of mTOR in translation. Semin Cell Dev Biol. 36:102–112.2014; [PubMed: 25263010]

9. Park KK, et al. Promoting Axon Regeneration in the Adult CNS by Modulation of the PTEN/mTOR Pathway. Science. 322:963–966.2008; [PubMed: 18988856]

10. Abe N, Borson SH, Gambello MJ, Wang F, Cavalli V. Mammalian target of rapamycin (mTOR) activation increases axonal growth capacity of injured peripheral nerves. J Biol Chem. 285:28034–28043.2010; [PubMed: 20615870]

11. Duan X, et al. Subtype-specific regeneration of retinal ganglion cells following axotomy: effects of osteopontin and mTOR signaling. Neuron. 85:1244–1256.2015; [PubMed: 25754821]

12. Chen W, et al. Rapamycin-Resistant mTOR Activity Is Required for Sensory Axon Regeneration Induced by a Conditioning Lesion. eNeuro. 3:e0358-0316.2016 0351–0317.2016;

13. Raab-Graham KF, Haddick PC, Jan YN, Jan LY. Activity- and mTOR-dependent suppression of Kv1.1 channel mRNA translation in dendrites. Science. 314:144–148.2006; [PubMed: 17023663]

14. Sosanya NM, et al. Degradation of high affinity HuD targets releases Kv1.1 mRNA from miR-129 repression by mTORC1. J Cell Biol. 202:53–69.2013; [PubMed: 23836929]

15. Kye MJ, et al. SMN regulates axonal local translation via miR-183/mTOR pathway. Hum Mol Genet. 23:6318–6331.2014; [PubMed: 25055867]

16. Gracias NG, Shirkey-Son NJ, Hengst U. Local translation of TC10 is required for membrane expansion during axon outgrowth. Nat Commun. 5:3506.2014; [PubMed: 24667291]

17. Meyuhas O. Ribosomal Protein S6 Phosphorylation: Four Decades of Research. Int Rev Cell Mol Biol. 320:41–73.2015; [PubMed: 26614871]

18. Saxton RA, Sabatini DM. mTOR Signaling in Growth, Metabolism, and Disease. Cell. 168:960–976.2017; [PubMed: 28283069]

19. Smith DS, Skene JH. A transcription-dependent switch controls competence of adult neurons for distinct modes of axon growth. J Neurosci. 17:646–658.1997; [PubMed: 8987787]

20. Forester CM, et al. Revealing nascent proteomics in signaling pathways and cell differentiation. Proc Natl Acad Sci U S A. 2018

21. Rishal I, et al. Axoplasm isolation from peripheral nerve. Dev Neurobiol. 70:126–133.2010; [PubMed: 19885832]

22. Perry, Rotem B-T; , et al. Subcellular Knockout of Importin β1 Perturbs Axonal Retrograde Signaling. Neuron. 75:294–305.2012; [PubMed: 22841314]

23. Perry RB, et al. Nucleolin-Mediated RNA Localization Regulates Neuron Growth and Cycling Cell Size. Cell Rep. 16:1664–1676.2016; [PubMed: 27477284]

24. Gandin V, et al. nanoCAGE reveals 5′ UTR features that define specific modes of translation of functionally related MTOR-sensitive mRNAs. Genome Res. 26:636–648.2016; [PubMed: 26984228]

25. Meyuhas O, Kahan T. The race to decipher the top secrets of TOP mRNAs. Bba-Gene Regul Mech. 1849:801–811.2015;

26. Rishal I, Fainzilber M. Axon-soma communication in neuronal injury. Nat Rev Neurosci. 15:32–42.2014; [PubMed: 24326686]

27. Ben-Yaakov K, et al. Axonal transcription factors signal retrogradely in lesioned peripheral nerve. EMBO J. 31:1350–1363.2012; [PubMed: 22246183]

28. Andreassi C, Riccio A. To localize or not to localize: mRNA fate is in 3′UTR ends. Trends Cell Biol. 19:465–474.2009; [PubMed: 19716303]

29. Kobayashi M, Wilson AC, Chao MV, Mohr I. Control of viral latency in neurons by axonal mTOR signaling and the 4E-BP translation repressor. Genes Dev. 26:1527–1532.2012; [PubMed: 22802527]

30. Ebrahimi-Fakhari D, et al. Impaired Mitochondrial Dynamics and Mitophagy in Neuronal Models of Tuberous Sclerosis Complex. Cell Rep. 17:1053–1070.2016; [PubMed: 27760312]

31. Younts TJ, et al. Presynaptic Protein Synthesis Is Required for Long-Term Plasticity of GABA Release. Neuron. 92:479–492.2016; [PubMed: 27764673]

32. Betz C, Hall MN. Where is mTOR and what is it doing there? J Cell Biol. 203:563–574.2013; [PubMed: 24385483]

33. Sancak Y, et al. Ragulator-Rag complex targets mTORC1 to the lysosomal surface and is necessary for its activation by amino acids. Cell. 141:290–303.2010; [PubMed: 20381137]

34. Ebner M, Sinkovics B, Szczygiel M, Ribeiro DW, Yudushkin I. Localization of mTORC2 activity inside cells. J Cell Biol. 216:343–353.2017; [PubMed: 28143890]

35. Feng G, et al. Imaging neuronal subsets in transgenic mice expressing multiple spectral variants of GFP. Neuron. 28:41–51.2000; [PubMed: 11086982]

36. Rishal I, et al. A motor-driven mechanism for cell-length sensing. Cell Rep. 1:608–616.2012; [PubMed: 22773964]

37. Schmidt EK, Clavarino G, Ceppi M, Pierre P. SUnSET, a nonradioactive method to monitor protein synthesis. Nat Methods. 6:275–277.2009; [PubMed: 19305406]

38. Harris VM. Protein detection by Simple Western analysis. Methods Mol Biol. 1312:465–468.2015; [PubMed: 26044028]

39. Soderberg O, et al. Direct observation of individual endogenous protein complexes in situ by proximity ligation. Nat Methods. 3:995–1000.2006; [PubMed: 17072308]

40. tom Dieck S, et al. Direct visualization of newly synthesized target proteins in situ. Nat Methods. 12:411–414.2015; [PubMed: 25775042]

41. Urisman A, et al. An Optimized Chromatographic Strategy for Multiplexing In Parallel Reaction Monitoring Mass Spectrometry: Insights from Quantitation of Activated Kinases. Mol Cell Proteomics. 16:265–277.2017; [PubMed: 27940637]

42. Doll S, Urisman A, Oses-Prieto JA, Arnott D, Burlingame AL. Quantitative Proteomics Reveals Fundamental Regulatory Differences in Oncogenic HRAS and Isocitrate Dehydrogenase (IDH1) Driven Astrocytoma. Mol Cell Proteomics. 16:39–56.2017; [PubMed: 27834733]

43. MacLean B, et al. Skyline: an open source document editor for creating and analyzing targeted proteomics experiments. Bioinformatics. 26:966–968.2010; [PubMed: 20147306]

44. Chalkley RJ, et al. Comprehensive analysis of a multidimensional liquid chromatography mass spectrometry dataset acquired on a quadrupole selecting, quadrupole collision cell, time-of-flight mass spectrometer: II. New developments in Protein Prospector allow for reliable and comprehensive automatic analysis of large datasets. Mol Cell Proteomics. 4:1194–1204.2005; [PubMed: 15937296]

45. Titov DV, et al. XPB, a subunit of TFIIH, is a target of the natural product triptolide. Nat Chem Biol. 7:182–188.2011; [PubMed: 21278739]

46. Vuppalanchi D, et al. Conserved 3′-untranslated region sequences direct subcellular localization of chaperone protein mRNAs in neurons. J Biol Chem. 285:18025–18038.2010; [PubMed: 20308067]

47. Spillane M, Ketschek A, Merianda TT, Twiss JL, Gallo G. Mitochondria coordinate sites of axon branching through localized intra-axonal protein synthesis. Cell Rep. 5:1564–1575.2013; [PubMed: 24332852]

48. Kalinski AL, et al. mRNAs and Protein Synthetic Machinery Localize into Regenerating Spinal Cord Axons When They Are Provided a Substrate That Supports Growth. J Neurosci. 35:10357–10370.2015; [PubMed: 26180210]

49. Sachdeva R, Farrell K, McMullen MK, Twiss JL, Houle JD. Dynamic Changes in Local Protein Synthetic Machinery in Regenerating Central Nervous System Axons after Spinal Cord Injury. Neural Plast. 2016:4087254.2016; [PubMed: 27375904]

50. Hu JK, et al. An FAK-YAP-mTOR Signaling Axis Regulates Stem Cell-Based Tissue Renewal in Mice. Cell Stem Cell. 21:91–106 e106.2017; [PubMed: 28457749]

51. Li Q, et al. Fbxl4 Serves as a Clock Output Molecule that Regulates Sleep through Promotion of Rhythmic Degradation of the GABAA Receptor. Curr Biol. 27:3616–3625 e3615.2017; [PubMed: 29174887]

52. Ran FA, et al. Genome engineering using the CRISPR-Cas9 system. Nat Protoc. 8:2281–2308.2013; [PubMed: 24157548]

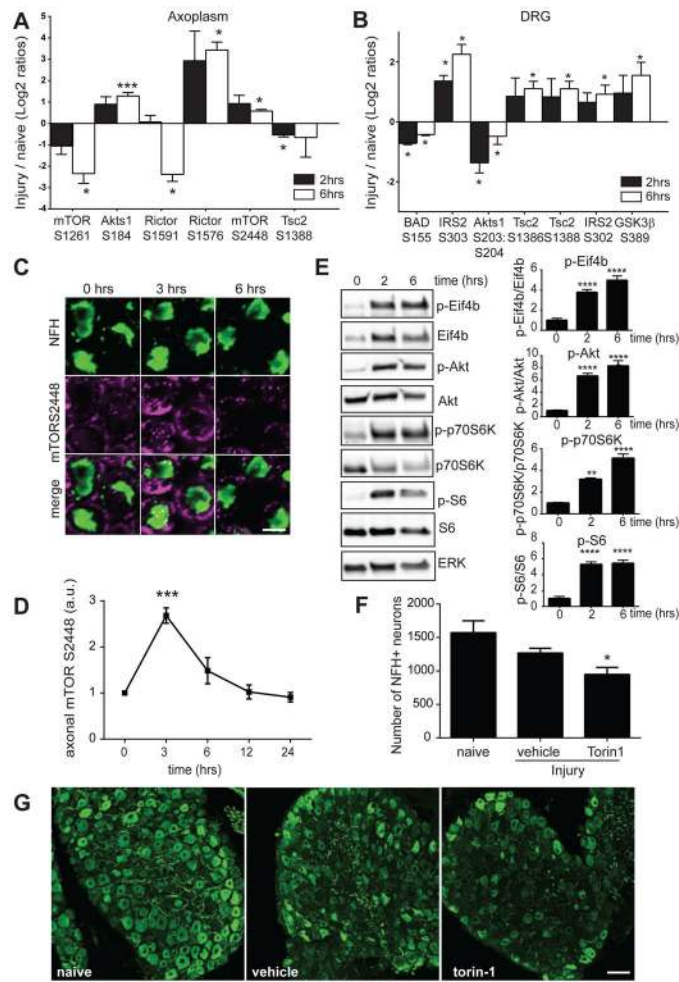**Fig. 1. mTOR activation after nerve injury**

(A) mTOR pathway phosphorylations significantly regulated by SN injury. n=3, * p < 0.05, *** p < 0.005, t-test. **(B)** As in A for L4/L5 DRG. n=3, * p < 0.05, t-test. **(C)** SN sections stained for the axonal marker NFH (green) and mTORS2448 (magenta), naive versus 3 and 6 hr after injury. Scale bar 5 μm. **(D)** Axonal mTORS2448 over time after injury, normalized to naive (n = 3, *** p < 0.005, one way ANOVA with Bonferroni's post-test). **(E)** Immunoblots of phospho-EIF4b, Akt, S6K, and S6 and the corresponding total proteins in SN axoplasm over time after injury. Quantifications on the right (n = 4, * p < 0.05, ** p < 0.001, one way ANOVA with Bonferroni's post-test). **(F, G)** SNs were injected with vehicle or Torin-1 prior to injury and L4 DRG were harvested 7 days later, serially sectioned at 20 μm intervals, and stained for NFH (green) to allow counting of proprioceptive neurons. Quantifications of NFH-positive neuron numbers per DRG are shown in F (n = 7, * p < 0.05, t-test), representative images are in G (scale bar 50 μm).
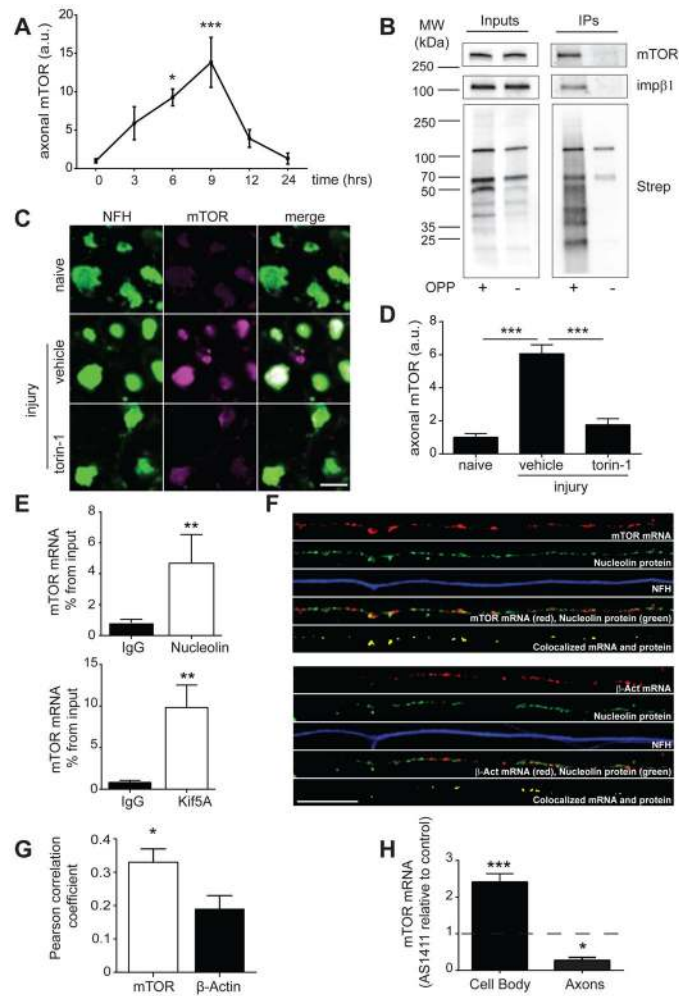
Fig. 2. mTOR is locally translated after SN injury

(**A**) mTOR regulation over time after injury at the SN lesion site (n = 5, * p< 0.05, *** p<0.005, one way ANOVA with Bonferroni's post-test). (**B**) Immunoblots reveal newly synthesized mTOR and Impβ1 from OPP treated rat SNs, confirming their local translation after injury. (**C**) Torin-1 (4 μM) effects on mTOR upregulation in sections from SN 4 hr ex vivo, stained for NFH (green) and mTOR (magenta). Scale bar 5 μm. (**D**) Quantification of axonal mTOR from C (n = 6, *** p < 0.005, one way ANOVA with Bonferroni's post-test). (**E**) Quantification of mTOR transcript levels after pull down for Kif5A or nucleolin in axoplasm (n = 6), % from input, Mean ± SEM, ** denotes p < 0.01 (ratio paired t-test). (**F**) Representative epifluorescent images for co-localization of endogenous mTOR or β actin transcripts visualized by in situ hybridization (red) and nucleolin protein visualized by immunostaining (green). Axons were visualized by neurofilament immunostaining (blue). Scale bar 10 μm. (**G**) Pearsons correlation coefficient for mTOR mRNA colocalization with nucleolin (0.33 ± 0.04, n = 24) differs significantly from that of β actin mRNA colocalization with nucleolin (0.19 ± 0.04, n = 20). * denotes p < 0.05 (t-test). (**H**) Quantification of relative mTOR transcript levels in cell bodies and axons of neurons treated with AS1411 versus control aptamer, plotted as a fold change over control aptamer. 18S

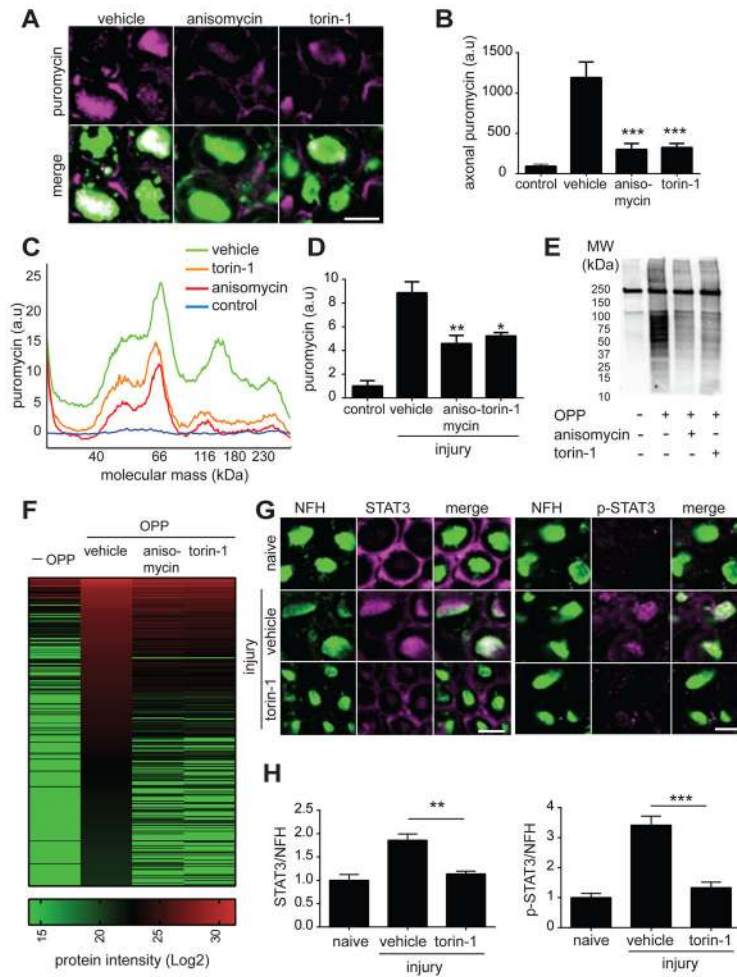RNA served as an internal control. Mean ± SEM, n=3, * denotes $p < 0.05$ (unpaired two sample t-test).

Fig. 3. mTOR regulates axonal local translation after SN injury

(A) SN segments 2 hr *ex vivo* with anisomycin (200 μg/ml), torin-1 (4 μM) or vehicle, followed by 1 hr puromycin (100 μg/ml), sectioned and stained for NFH (green) and puromycin (magenta). Scale bar 5 μm. **(B)** Quantification of axonal puromycin in experiment described in A (n = 5, *** $p < 0.001$, one way ANOVA with Bonferroni's post-test). **(C)** Representative runs of puromycinylated proteins in SN axoplasm from experiment described in A analysed by capillary immunoelectrophoresis. **(D)** Quantification of C (n=4, * $p < 0.05$, ** $p < 0.01$, ANOVA with Bonferroni post-test). **(E)** SA-HRP immunoblots of OPP-biotin labeled axoplasm samples prior to MS. **(F)** Heat map of OPP-biotin labeled protein candidates identified by MS. **(G)** SN segments 4 hr ex vivo with Torin-1 (4 μM) or vehicle (DMSO), sectioned and stained for NFH (green) and STAT3 or phosphorylated STAT3 (pSTAT3, both magenta). Scale bars 5 μm. **(H)** Quantification of axonal STAT3 and p-STAT3 for the experiment described in G (n = 4, ** $p < 0.01$, *** $p < 0.005$, one way ANOVA with Bonferroni's post-test).
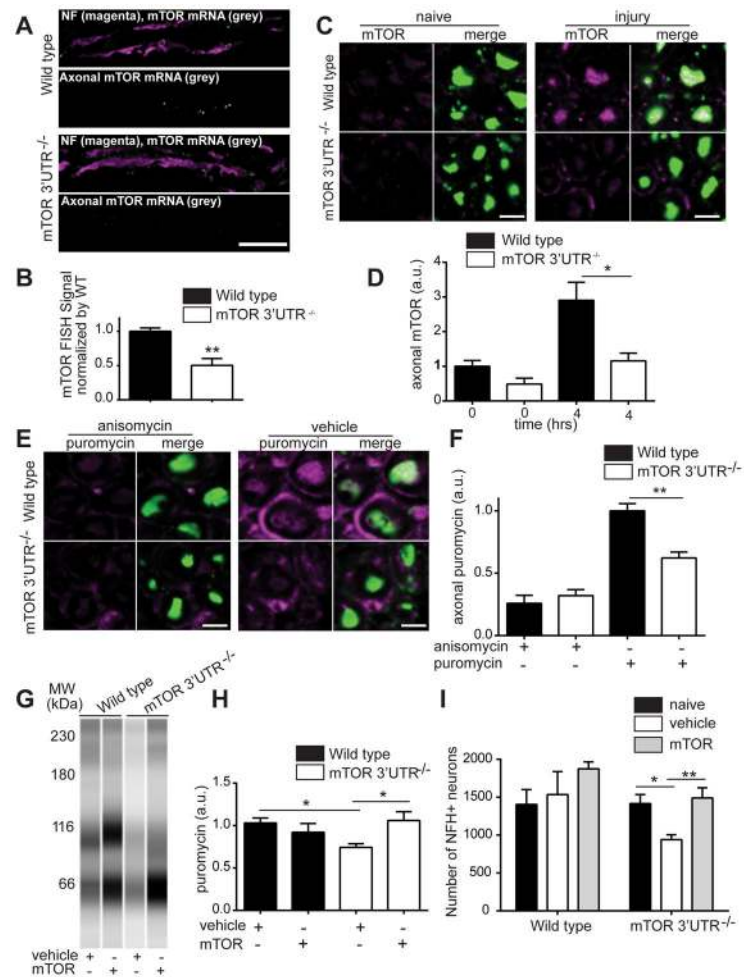
Fig. 4. Effects of mTOR 3′UTR deletion

(**A**) Representative, exposure-matched confocal images of Stellaris FISH for mTOR mRNA and neurofilament (NF) immunostaining from SN sections of wild type and mTOR 3′UTR $^{-/-}$ mice. Upper panels show single optical planes for merged NFH and mTOR channels. Lower panels show single optical planes of mTOR mRNA pixels that overlap with NFH and were projected to a separate channel as 'axon only' mTOR signals. Scale bar 10 μm. (**B**) Quantification of A reveals approximately 50% reduction in axonal mTOR in the 3′UTR$^{-/-}$ mice (n = 4, ** p < 0.01, unpaired t-test). (**C**) SN segments from the indicated genotypes 4 hr ex vivo, sectioned and stained for NFH (green) and mTOR (magenta). Scale bar 5 μm. (**D**) Quantification of C (n = 3, * p < 0.05, one way ANOVA with Bonferroni's post-test). (**E**) SN segments from the indicated genotypes 2 hr ex vivo with anisomycin (200 μg/ml) or vehicle, followed by 1 hr puromycin (100 μg/ml), then sectioned and stained as indicated. Scale bar 5 μm. (**F**) Quantification of E (n = 3, ** p < 0.01, one way ANOVA with Bonferroni's post-test). (**G**) SN segments from wild type and mTOR 3′UTR$^{-/-}$ mice not injected, injected with vehicle and injected with 350 ng mTOR protein were incubated in DMEM 2 hr ex vivo, followed by 1 hr puromycin (100 μg/ml) treatment. A representative pseudo-blot of puromycinylated proteins in SN axoplasm analysed by capillary immunoelectrophoresis is shown. (**H**) Quantification of G (n=4, *** p< 0.005, one way

ANOVA with Bonferroni's post-test). **(I)** SNs from wild type and mTOR 3′UTR$^{-/-}$ mice were injected with either vehicle or 350 ng of mTOR protein concomitant with crush injury. L4 DRGs connected to the injured sciatic were harvested 7 days after injury, serially sectioned at 20 μm intervals and stained for the proprioceptive marker NFH. Naive L4 DRG were also processed as a reference. Number of NFH positive neurons per DRG (n = 4, * $p < 0.05$, ** $p < 0.01$, one way ANOVA with Tukey's post-test).